Pediatr Radiol (2012) 42 (Suppl 1):S62–S73
DOI 10.1007/s00247-011-2171-7

Imaging of fetal chest masses

Richard A. Barth

Received: 25 January 2011 / Revised: 25 February 2011 / Accepted: 12 March 2011

Abstract Prenatal imaging with high-resolution US and rapid acquisition MRI plays a key role in the accurate diagnosis of congenital chest masses. Imaging has enhanced our understanding of the natural history of fetal lung masses, allowing for accurate prediction of outcome, parental counseling, and planning of pregnancy and newborn management. This paper will focus on congenital bronchopulmonary malformations, which account for the vast majority of primary lung masses in the fetus. In addition, anomalies that mimic masses and less common causes of lung masses will be discussed.

Keywords Fetal imaging · Fetal chest mass · Bronchopulmonary malformation · Congenital diaphragmatic hernia

Bronchopulmonary malformations

Congenital bronchopulmonary malformations (BPMs) represent a spectrum of lung anomalies, including congenital pulmonary airway malformation (frequently referred to as CCAM), bronchopulmonary sequestration (BPS), and congenital lobar overinflation (CLO). There is a growing consensus in the pathology literature that BPMs represent a spectrum of lesions caused by an airway obstructive malformation sequence and the specific type of malformation depends on the severity and timing of airway obstruction during fetal lung development [1–3]. Supporting this conclusion is the pathological diagnosis of bronchial atresia as a common association with the above-mentioned bronchopulmonary malformations [3].

In the pre-sonographic era, the majority of congenital lung masses presented postnatally with respiratory distress or pneumonia secondary to pulmonary compromise associated with a large mass (Fig. 1). The lesions often required acute medical or surgical treatment via intubation and/or immediate surgical resection. In the pre-sonographic era, the majority of congenital lung masses are detected on prenatal ultrasound as an incidental finding in the second or third trimester of pregnancy (Fig. 2). Prenatal diagnosis has improved our understanding of the natural history of congenital lung masses and plays a key role in pregnancy management decisions and family counseling regarding likely outcomes.

Congenital pulmonary airway malformations (CPAM)

CPAMs are the most common cause of prenatally diagnosed bronchopulmonary malformations, accounting for approximately half of all lesions (Table 1) [4]. A CPAM results from early airway maldevelopment and represents a benign hamartoma or dysplastic tumor, which are usually characterized by the presence of macrocystic or microcystic components. Stocker has pathologically classified CPAMs according to cyst size and resemblance to the segments of the developing bronchial tree and air spaces [5]. The term congenital pulmonary airway malformation is preferable to the term congenital cystic adenomatoid malformation as the lesions are cystic in only three of the five pathological classifications and adenomatoid in only one type [5]. CPAMs often communicate with the airways, although the

R. A. Barth (✉)
Department of Radiology, Lucile Packard Children's Hospital,
Stanford University School of Medicine,
725 Welch Road, Room 1690,
Stanford, CA 94305–5913, USA
e-mail: rabarth@stanford.edu

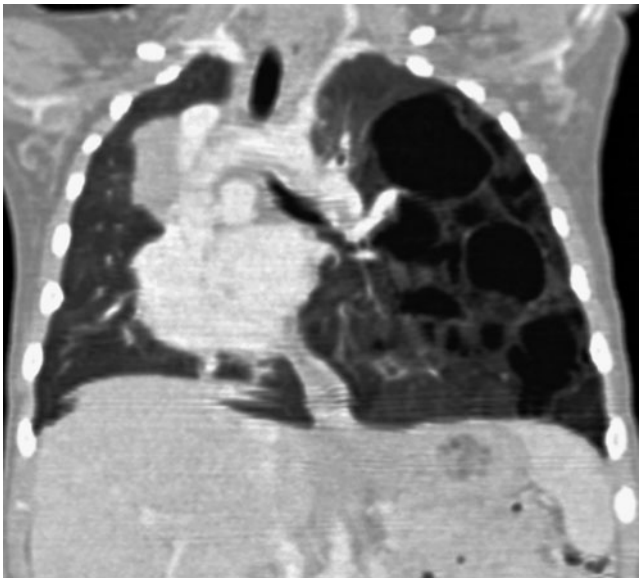

Fig. 1 Infant with respiratory distress secondary to congenital pulmonary airway malformation. Coronal plane CT scan of the chest shows a large macrocystic mass in the left chest resulting in mediastinal shift to the right

communication is abnormal. CPAMs receive their blood supply from the pulmonary artery and drain via the pulmonary veins with the exception of hybrid lesions (CPAM and sequestration), which also have a systemic arterial blood supply. The macrocystic lesions contain single or multiple cysts that are 5 mm or larger in diameter

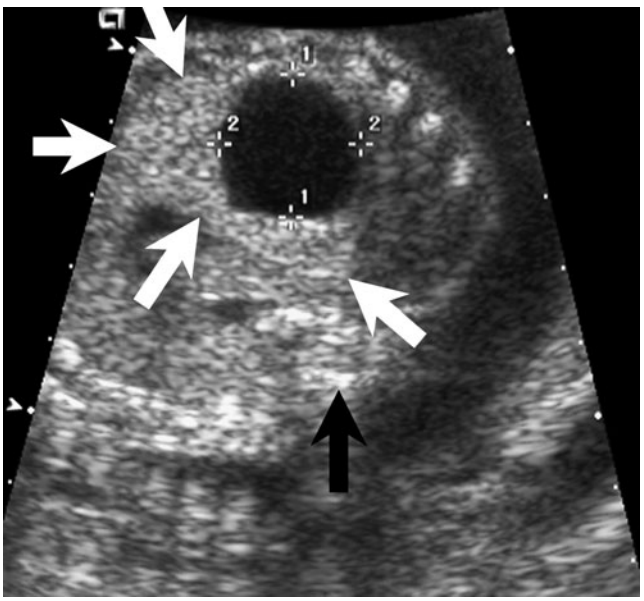

Fig. 2 Complex cystic lung mass detected as incidental finding on US at 22 weeks' gestational age. Axial sonogram through the fetal chest shows a complex mass composed of macrocystic (*calipers*) and solid (*white arrows*) components. Postnatal resection confirmed congenital pulmonary airway malformation. Fetal spine (*black arrow*)

Table 1 Distribution of pathologically proven fetal lung lesions (108 cases)[a]

CPAM	47%
Hybrid (CPAM and sequestration)	25%
Overinflation/bronchial atresia	20%
Sequestration	8%

[a] Adapted from Epelman et al. [4]

and the microcystic lesions appear as a solid mass on imaging.

Bronchopulmonary sequestration (BPS)

BPS is the second most common cause of a congenital lung mass, accounting for approximately 33% of all lesions (Table 2) [4]. BPS masses are commonly hybrid lesions with histological components of both sequestration and CPAM. BPS masses are composed of nonfunctioning lung tissue, do not have a connection to the tracheobronchial tree and are supplied by an anomalous systemic artery arising from the lower thoracic or upper abdominal aorta [6]. The majority of lesions are intrathoracic, usually in the lower lobes and on the left side [7–9]. Approximately 15% of sequestrations are intradiaphragmatic or subdiaphragmatic in location, most commonly on the left side of the abdomen [8, 10]. Two types of sequestrations have been described: intralobar and extralobar. Extralobar sequestrations have their own pleural investment and drain into systemic veins, whereas intralobar sequestrations share the pleural investment with the normal lung and usually drain into the pulmonary venous system [11]. Extralobar sequestrations may be associated with other congenital anomalies including congenital diaphragmatic hernia, cardiac abnormalities or foregut duplication cysts [12]. On imaging, the majority of sequestrations appear as solid masses, although cystic components can be seen within hybrid lesions. The subdiaphragmatic form of sequestration may mimic neuroblastoma or adrenal hemorrhage.

Congenital lobar overinflation (CLO)

CLO (a.k.a. congenital lobar emphysema) is an overinflation of a lung segment or lobe that on microscopic analysis is characterized by air space enlargement without maldevelopment [2]. Although the lung is hyperinflated, the alveolar walls remain intact; therefore, the term overinflation is preferred to that of emphysema. There is an evolving recognition of two subgroups of CLO. The first group historically presented with respiratory distress with an

Table 2 Imaging features seen in bronchopulmonary malformations

Imaging feature	CPAM	Sequestration	Lobar overinflation
Solid mass	Yes	Yes	Yes
Macroscopic cysts	Yes	Uncommon	No
Systemic arterial supply	No (exception: hybrid lesions)	Yes	No
Isolated pleural effusion	Uncommon	Yes	No
Systemic venous drainage	No	Yes (extralobar sequestration)	No

overinflated lung occurring secondary to intrinsic cartilage abnormality of the airway, absent bronchial cartilage or extrinsic compression of an airway by an enlarged pulmonary artery or bronchogenic cyst [13]. The collapsed airway acts as a one-way valve and results in air trapping. This subgroup of CLO most commonly involves the left upper lobe followed by the right middle and right upper lobes; the lower lobes are involved in less than 1% of cases [14]. A second subgroup of CLO is now being detected with increasing frequency as a result of prenatal imaging. The second group is characterized by segmental or lobar hyperinflation and a high association with bronchial atresia. This subgroup has a predisposition to involve the lower lobes [4, 15]. On prenatal imaging, CLO may appear similar to a microcystic CPAM, but unlike CPAM, fetal complications and postnatal sequelae are rare [15]. This subgroup is usually asymptomatic at birth [15].

Imaging of bronchopulmonary malformations

A BPM appears as a cystic, solid or complex mass on US (Fig. 2). Solid masses appear hyperechogenic compared to the normal fetal lung in the second trimester and often become isoechoic with the normal fetal lung and invisible in the third trimester (Fig. 3). The latter relates to the increasing echogenicity of the normal fetal lungs as pregnancy progresses, resulting in diminished conspicuity of a lung mass and the propensity of solid masses to decrease in size. When solid masses are isoechoic to normal lung, the diagnosis is more challenging and the ultrasonographer relies on mass effect, including mediastinal shift, altered cardiac position or axis, or an inverted diaphragm to confirm the diagnosis (Fig. 4). An echogenic solid fetal lung mass is not indicative of a specific diagnosis and can represent a microcystic CPAM, sequestration, congenital lobar or segmental overinflation, or congenital diaphragmatic hernia. Accurate diagnosis of a BPM is important since the reported complications of hydrops fetalis and pulmonary hypoplasia are most often associated with CPAM and are less likely to occur with the other causes of bronchopulmonary malformations. The most useful imaging features for differentiating solid fetal chest masses are as follows: (1) macroscopic cysts within a mass strongly indicate CPAM (Fig. 2); (2) systemic arterial blood supply to a lung mass confirms sequestration (Fig. 5); (3) a large pleural effusion associated with a mass favors a torsed sequestration (Fig. 6) (Table 1). BPS is usually located in the lower thorax, left side greater than right. A subset of sequestrations are subdiaphragmatic, usually on the left side, manifesting as a supra renal echogenic solid mass (Fig. 7).

MRI plays an important complementary role to US in the evaluation of congenital lung masses. The normal fetal lungs demonstrate increasing relative signal intensity on fluid-sensitive sequences as pregnancy progresses secondary to the accumulation of fluid within the developing lungs

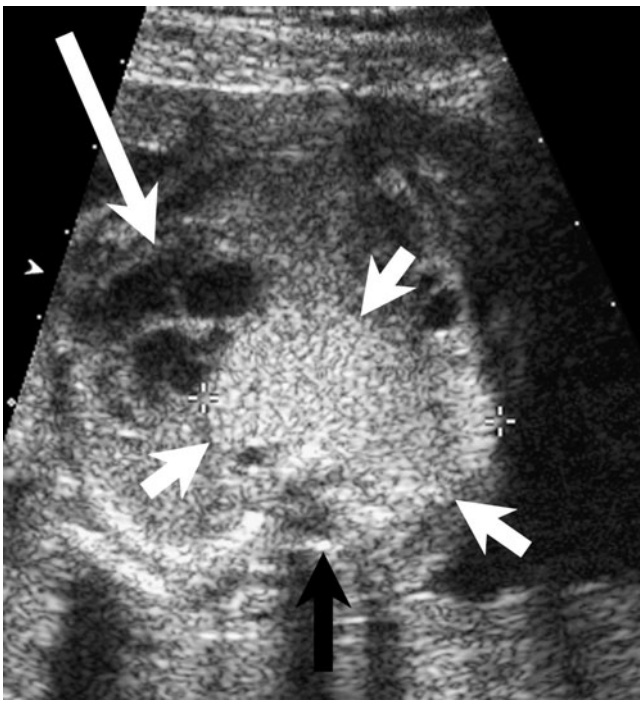

Fig. 3 Solid fetal chest mass at 22 weeks' gestational age. Axial sonogram of the fetal chest shows an echogenic solid mass (*short arrows*) in the left hemithorax. Heart (*long arrow*) is displaced into the right chest. Postnatal resection confirmed a congenital pulmonary airway malformation. Spine (*black arrow*)

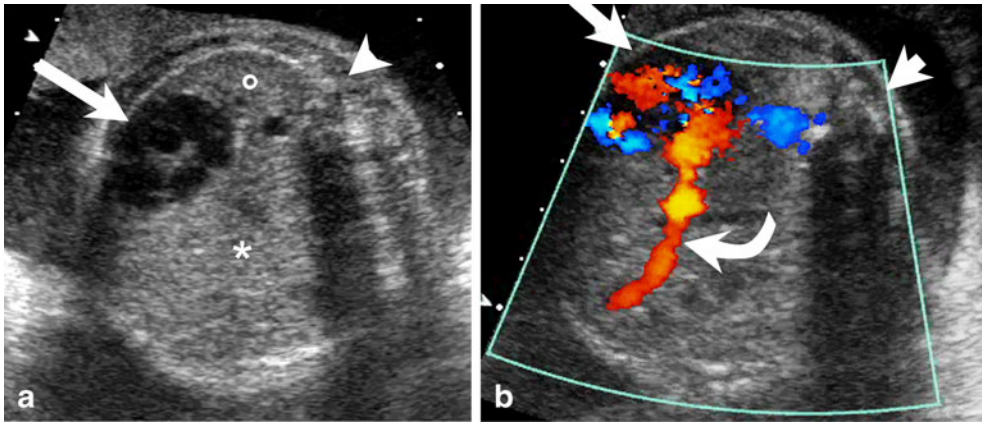

Fig. 4 Right congenital diaphragmatic hernia diagnosed at 26 weeks' gestational age. **a** Cardiac displacement (*arrow*) indicates the presence of a right-sided chest mass (*asterisk*) isoechoic to the normal fetal lung (*small circle*). Fetal spine (*arrowhead*). **b** Color Doppler axial sonogram through the fetal chest demonstrates the intrahepatic IVC (*curved arrow*) and liver in the right chest, confirming a right-side congenital diaphragmatic hernia. Fetal heart (*long arrow*). Fetal spine (*short arrow*)

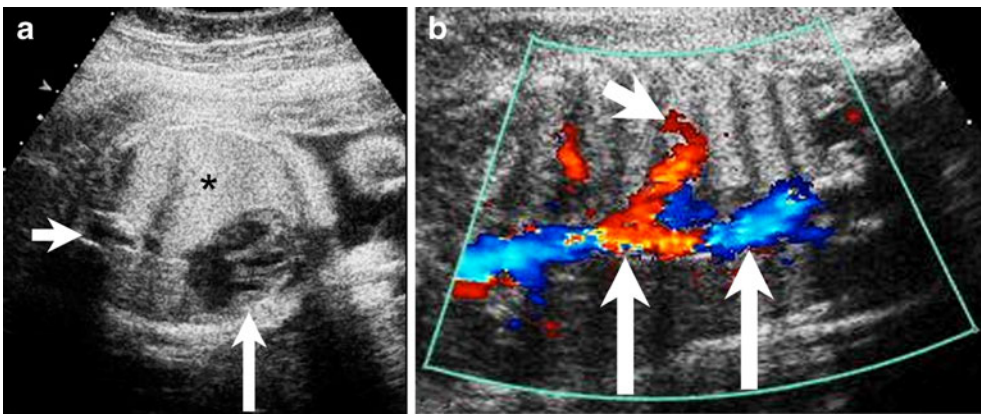

Fig. 5 Bronchopulmonary sequestration diagnosed at 22 weeks' gestational age. **a** Axial sonogram through the fetal chest shows a left-side solid chest mass (*asterisk*) displacing the heart (*long arrow*) to the right. Fetal spine (*short arrow*). **b** Coronal sonogram through the fetal chest and abdomen shows a systemic arterial feeder (*short arrow*) rising from the upper abdominal aorta (*long arrows*) to the fetal chest mass (**a**, *asterisk*)

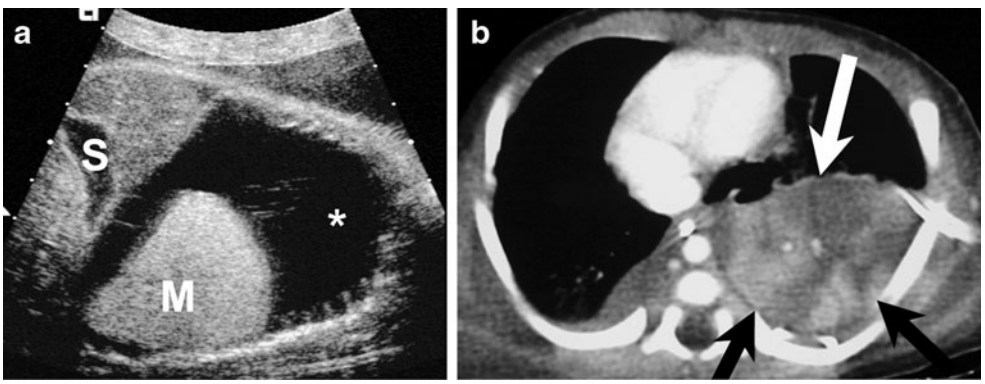

Fig. 6 Torsed sequestration diagnosed at 23 weeks' gestational age. **a** Parasagittal sonogram through the fetal chest and abdomen demonstrates a solid mass (*M*) surrounded by a large pleural effusion (*asterisk*). Stomach (*S*). **b** Axial CT of a newborn through the lower chest demonstrates heterogeneous necrotic torsed sequestration (*arrows*)

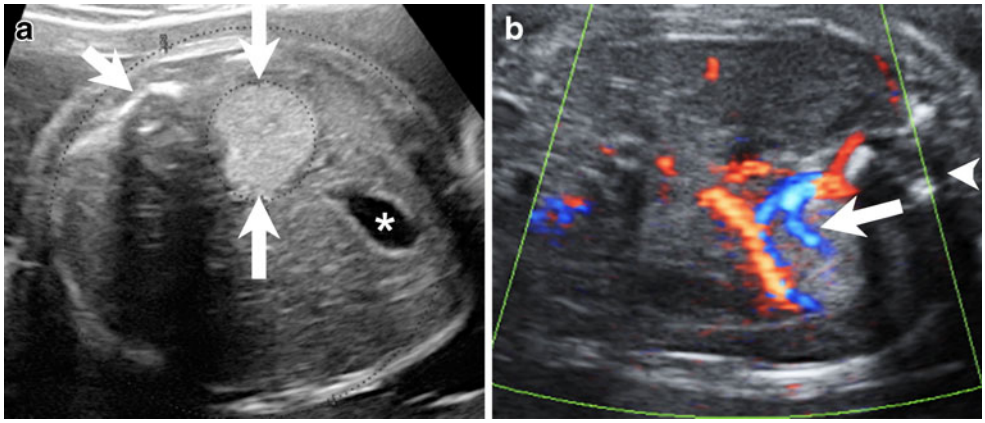

Fig. 7 Subdiaphragmatic bronchopulmonary sequestration at 25 weeks' gestational age. **a** Axial sonogram of the upper fetal abdomen demonstrates an echogenic solid left paraspinal mass (*long arrows*). Stomach (*asterisk*), spine (*short arrow*). **b** Color Doppler sonogram through the upper abdomen demonstrates systemic arterial blood supply from the celiac artery (*arrow*) into the subdiaphragmatic mass, confirming the diagnosis of bronchopulmonary sequestration. Spine (*arrowhead*)

[16, 17]. Most congenital lung malformations are higher signal than normal lungs in the second trimester on fluid-sensitive MR sequences (Fig. 8). Masses may appear iso-signal or lower signal compared to normal lung tissue in the third trimester of pregnancy. Similar to US, a high signal solid mass on MRI is not diagnostic for a specific type of BPM. The identification of a macroscopic cyst or systemic arterial blood supply to the mass improves specificity (Figs. 8 and 9) (Table 2) [18]. Pacharn et al. [18] reported high accuracy of prenatal MRI for diagnosing BPM and noted postnatal confirmation of the correct diagnosis on pathology or postnatal imaging in 96% of cases.

MRI provides alternative or additional diagnoses compared with US in 38–50% of fetuses (Fig. 10) [17, 19]. MRI complements US for equivocal chest masses or when the image quality is degraded secondary to maternal obesity. We have found MRI to be particularly useful when US shows dextroposition of the heart, which should always raise concern for an underlying lung mass displacing the heart. Cardiac dextroposition may also occur in the absence of a mass in association with right lung hypoplasia [20]. In the latter situation, MRI accurately excludes an underlying lung mass and confirms the diagnosis of pulmonary hypoplasia (Fig. 11). Right lung hypoplasia associated with cardiac dextroposition has a high association with cardiovascular anomalies, particularly, partial anomalous pulmonary venous return [20]. Therefore, all such cases should be assessed with a fetal cardiac echo examination.

Predicting outcome for bronchopulmonary malformations

Imaging plays a key role in predicting clinical outcome of fetuses diagnosed with BPM. The majority of fetuses with

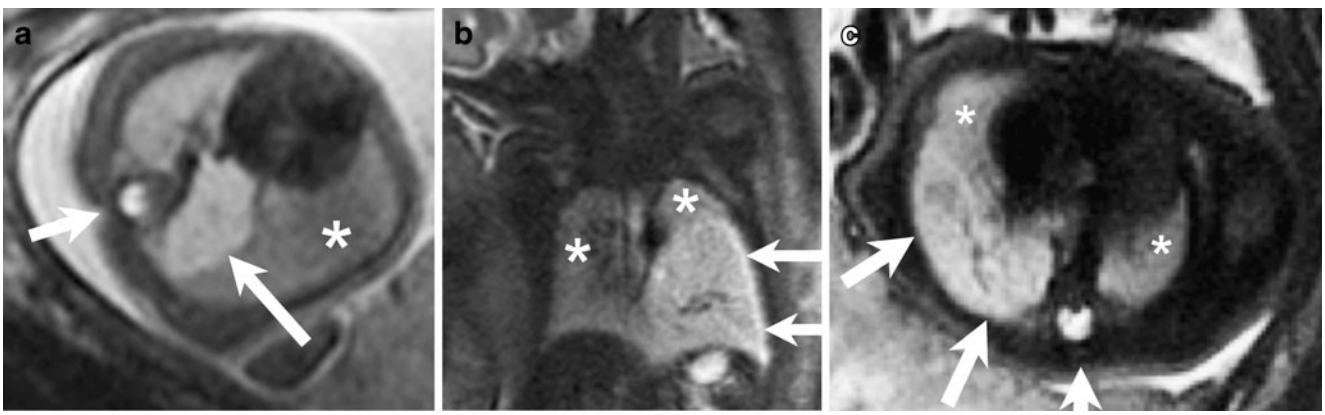

Fig. 8 Congenital lung masses are depicted on fluid-sensitive MR sequences. **a** Congenital pulmonary airway malformation at 22 weeks' gestational age. Axial plane MRI through the lower chest demonstrates a high signal mass (*long arrow*) adjacent to normal lung (*asterisk*). Spine (*short arrow*). **b** Bronchopulmonary sequestration at 22 weeks' gestational age. Coronal plane MRI demonstrates a large high signal mass (*arrows*) in the left chest. Normal lungs (*asterisks*). **c** Congenital lobar overinflation at 34 weeks' gestational age. Axial MRI demonstrates high signal mass (*arrows*) in the right lower chest. Normal lung (*asterisks*)

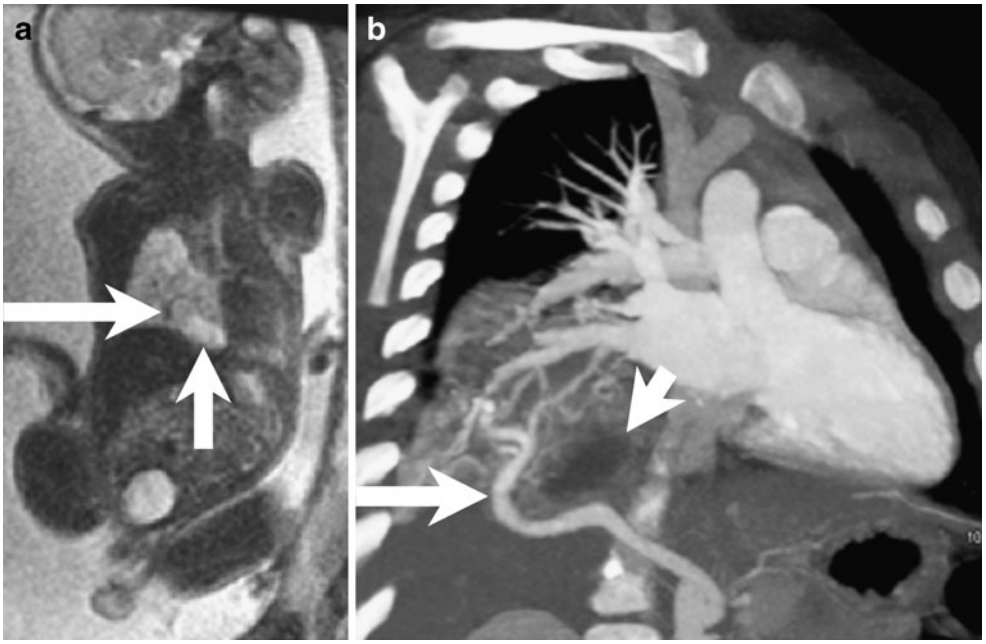

Fig. 9 Hybrid lung malformation (bronchopulmonary sequestration and congenital pulmonary airway malformation) at 28 weeks' gestational age. **a** Coronal plane MRI shows a high signal mass in the right chest with a systemic vessel (*long arrow*) coursing upward from the diaphragm into the mass. Macrocystic component (*short arrow*) suggests hybrid lesion. **b** Newborn CT angiogram. Coronal plane view confirms the systemic arterial feeder (*long arrow*) arising from the upper abdominal aorta and a fluid-filled macrocystic component (*short arrow*)

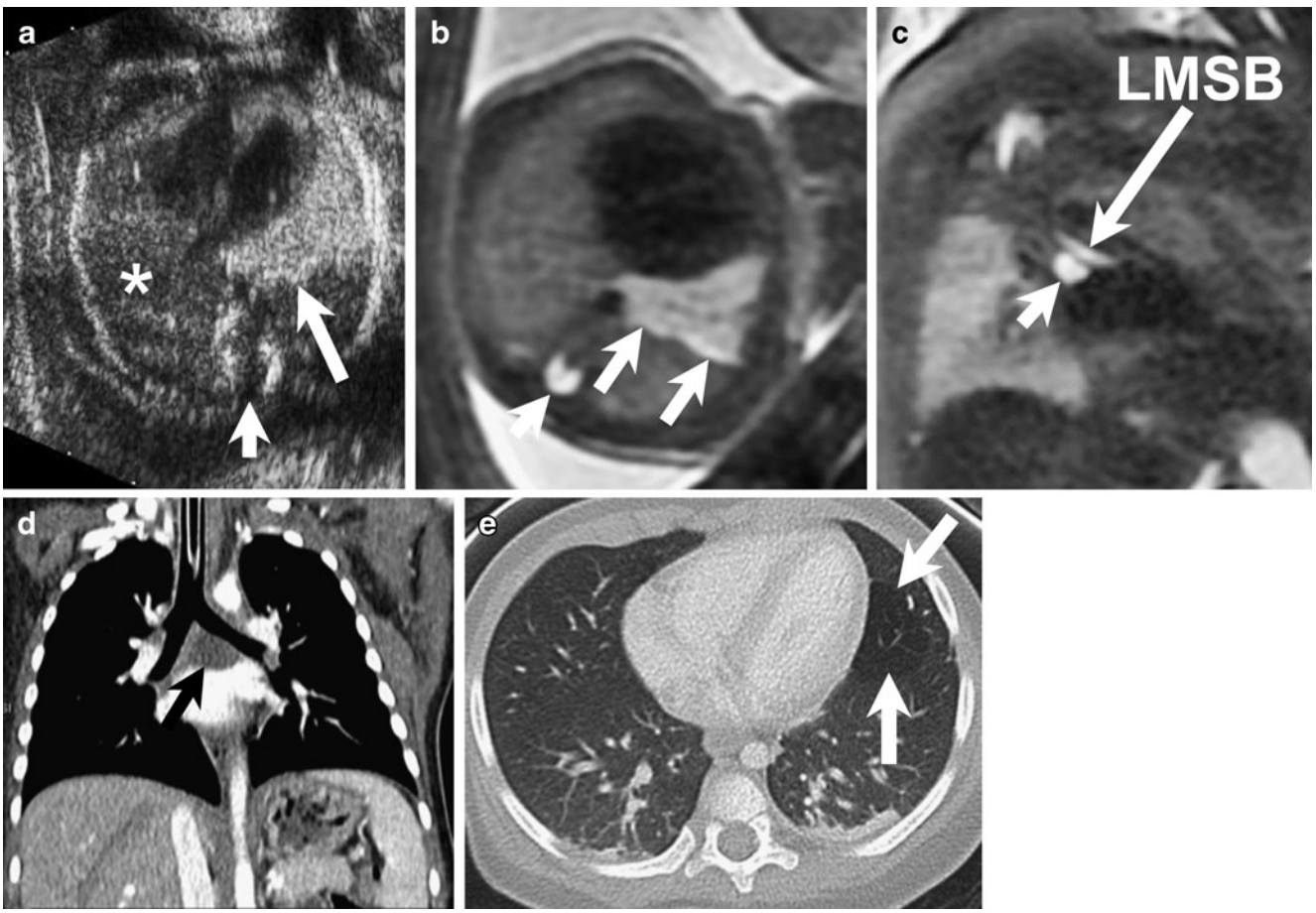

Fig. 10 Bronchogenic cyst causing lung overinflation at 23 weeks' gestational age. **a** Axial sonogram through the fetal chest demonstrates an echogenic solid mass (*long arrow*) in the left lingula. Normal lung (*asterisk*), fetal spine (*short arrow*). **b** Axial plane fetal MRI demonstrates high signal mass in left lingula (*arrows*). Fetal spine (*short arrow*). **c** Coronal plane MRI confirms subcarinal bronchogenic cyst (*short arrow*) as the likely cause of the lingula overinflation. *LMSB* = left main-stem bronchus (*long arrow*). **d** Coronal plane CT of the newborn confirms subcarinal bronchogenic cyst (*arrow*). **e** Axial plane CT scan shows segmental hyperinflation (*arrows*) within the lingula of the left lung

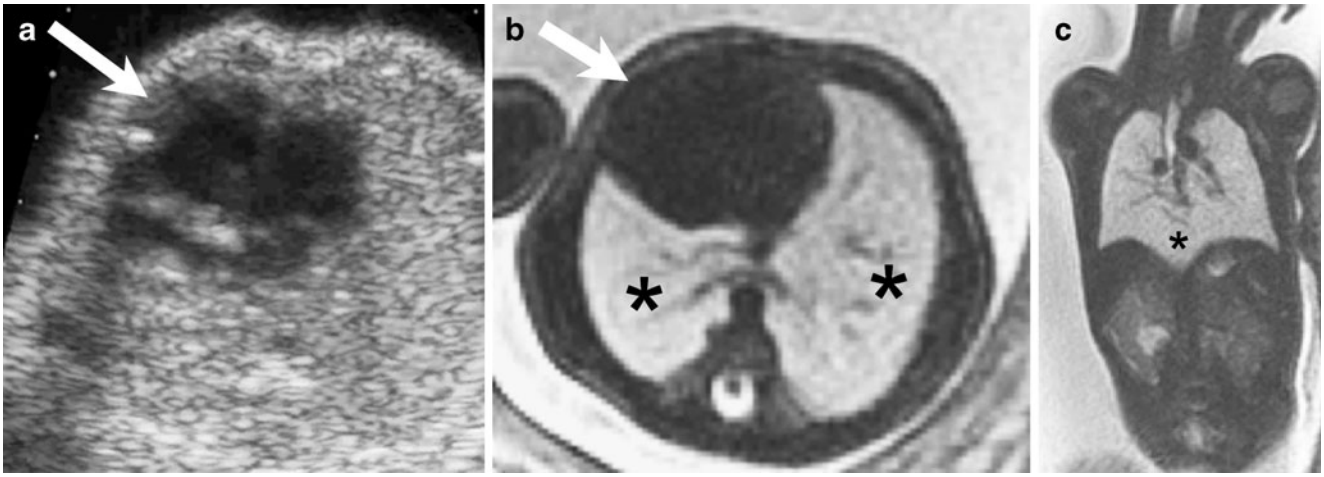

Fig. 11 Cardiac dextroposition associated with right pulmonary hypoplasia and horseshoe lung. **a** Axial sonogram through the fetal chest shows dextroposition of the heart (*arrow*). **b** Axial MRI through the fetal chest shows dextroposition of the heart (*arrow*) and normal lungs (*asterisks*) excluding an underlying lung mass. **c** Coronal plane MRI shows a horseshoe lung with the isthmus (*asterisk*) bridging the two lower lobes

an isolated BPM have an excellent prognosis and usually are asymptomatic at birth. Prognosis depends largely on the size of the mass and the presence or absence of hydrops fetalis. Small isolated fetal lung malformations with no mass effect have excellent outcomes. A subset of fetuses with large BPMs and mass effect resulting in mediastinal shift will develop life-threatening complications usually secondary to hydrops fetalis or less commonly severe pulmonary hypoplasia (Fig. 12). The vast majority of complications are described in association with CPAM (a.k.a. CCAM). Early literature reported that 30–50% of fetuses with CPAM develop hydrops with an associated mortality approaching 100% without intervention [21–23]. More recent literature suggests that hydrops is less frequent and occurs in 9–21% of cases [24, 25]. Hydrops is universally associated with large masses and occurs secondary to compression of the heart and inferior vena cava obstructing venous return to the heart. It is important to note that whereas hydrops is almost universally associated with a large fetal lung mass, only a minority of large lung masses will progress to hydrops. Large masses are also associated with isolated polyhydramnios secondary to compression of the esophagus obstructing the normal passage of amniotic fluid into the gastrointestinal tract. In a retrospective series, Crombleholme et al. [22] reported that sonographic measurement of a cystic adenomatoid malformation volume ratio (CVR) predicted the risk of hydrops in fetuses with CPAM (a.k.a. CCAM). CVR is the measured CPAM volume divided by the head circumference. A CVR greater than or equal to 1.6 predicted an increased risk for hydrops fetalis. A CVR less than or equal to 1.6 in the absence of a dominant cyst was associated with a less than a 3% risk for hydrops fetalis. Crombleholme et al. [22] suggested that in addition to absolute size of the mass, the rate of growth of the lesion, particularly when associated with a macroscopic cyst, is a risk factor for developing hydrops fetalis.

Approximately 40% of CPAMs increase in size during pregnancy, with the most rapid growth occurring 20–26 weeks' gestational age after which growth peaks and plateaus [22, 26]. Differentiation of CPAM from other BPMs is not always possible. Therefore, surveillance sonograms of all fetal chest masses are recommended in

Fig. 12 Fetal hydrops associated with large congenital pulmonary airway malformation at 21 weeks' gestational age. Coronal plane MRI demonstrates a large mass (*M*) in the left chest, inverting the left hemidiaphragm. Fetal ascites (*asterisk*)

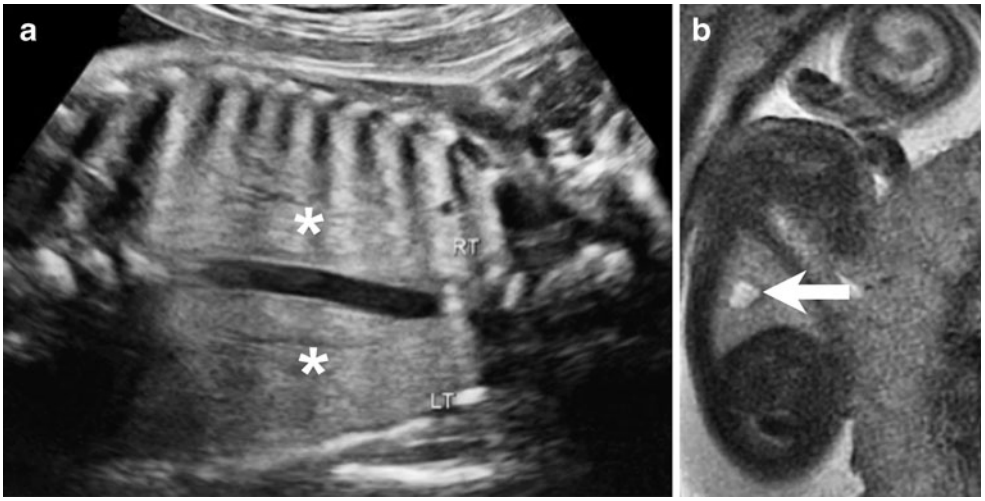

Fig. 13 Disappearing fetal lung mass in the third trimester. **a** Coronal plane sonogram through the fetal chest shows no evidence of a fetal lung mass. Normal lungs (*asterisks*). **b** Sagittal plane fetal MRI confirms small high-signal bronchopulmonary malformation (*arrow*)

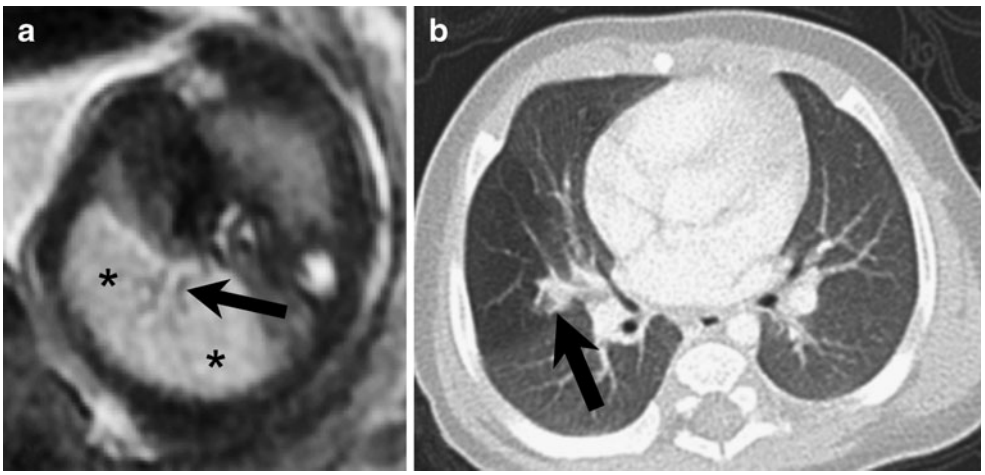

Fig. 14 Congenital lobar overinflation diagnosed at 22 weeks' gestational age. **a** Axial MRI scan through the fetal chest shows a right-side high signal mass (*asterisks*) and a central dilated bronchus (*arrow*) consistent with mucoid impaction. **b** Axial CT scan of the chest at 3 months of age confirms overinflation within the right lower lobe and central bronchial mucoid impaction (*arrow*) consistent with bronchial atresia

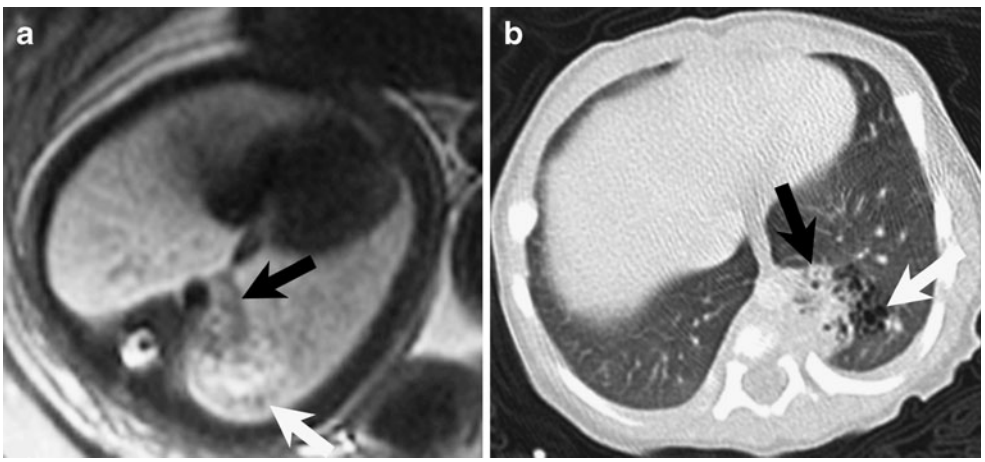

Fig. 15 Third trimester MRI correlates with newborn CT. **a** Axial plane MRI scan at 35 weeks' gestational age demonstrates solid (*black arrow*) and cystic (*white arrow*) components of a CPAM. **b** Axial CT scan at birth shows corresponding solid (*black arrow*) and cystic (*white arrow*) components of a CPAM

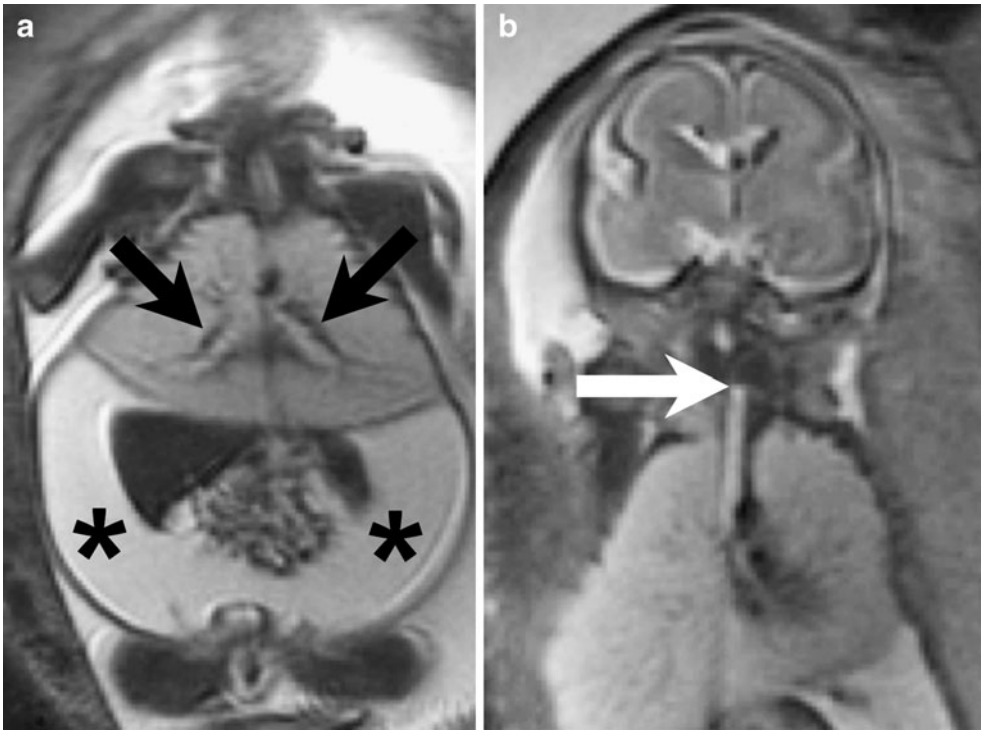

Fig. 16 Congenital high airway obstruction syndrome. **a** Coronal MRI through fetal chest at 25 weeks' gestational age shows the characteristic findings of hyperinflated lungs, dilated central bronchi (*arrows*) and fetal ascites (*asterisks*). **b** Coronal plane MRI sequence through the fetal chest demonstrates complete obstruction at the level of the larynx (*arrow*), which was confirmed postnatally to be secondary to laryngeal atresia

the second trimester because an initially small mass may progress to a large mass and pose a risk for hydrops fetalis. After 28 weeks' gestational age, the risk of developing hydrops fetalis is extremely low. Approximately 15% of CPAMs regress and disappear on US, usually in the third trimester (Fig. 13) [22]. US accurately diagnoses hydrops fetalis, which is typically defined as the presence of extracellular fluid in at least two compartments, including body wall edema, pericardial effusion, pleural effusion or ascites. When a fetus with a CPAM and a dominant cyst develops hydrops prior to 32 weeks' gestational age, cyst aspiration or thoraco-aminotic shunt may be considered in an attempt to reverse the hydrops. Thoraco-amniotic shunts are usually reserved for cases in which the cyst re-accumulates fluid quickly following cyst aspiration. For solid masses with hydrops, surgical resection may be considered prior to 32 weeks' gestational age as a life-saving intervention. Recently, high-dose maternal steroids have been reported to reverse hydrops associated with a fetal chest mass with survival rates ranging from 46% to 100% [27, 28]. After 32 weeks' gestation, many centers will consider delivery of a hydropic fetus as a potentially life-saving intervention. US accurately diagnoses fetal hydrops, but MRI may complement US in assessing the volume of normal residual lung tissue, particularly when a lung mass is large and the lungs are more difficult to assess on US. This may be important in predicting severe pulmonary hypoplasia associated with a large bronchopulmonary mass.

The prognosis for BPS is very good with the majority of lesions regressing in size during pregnancy and survival approaching 100% [9]. Rarely, extralobar sequestrations

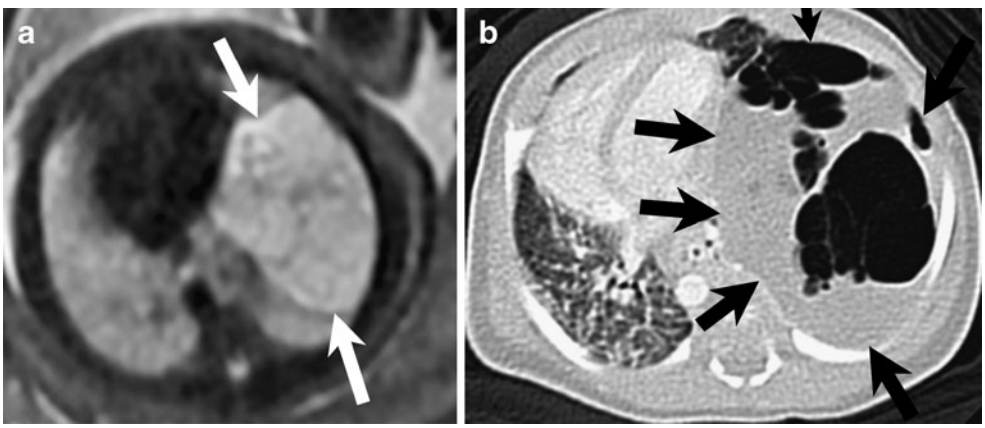

Fig. 17 Cystic pleuropulmonary blastoma. **a** Axial plane MRI demonstrates high signal mass (*arrows*) within the left fetal chest, displacing the heart to the right. **b** Axial CT scan after birth confirms a solid, air-containing cystic mass (*arrows*) proved surgically to represent a cystic pleuropulmonary blastoma (Courtesy of Beth Kline-Fath, M.D., Cincinnati Children's Hospital)

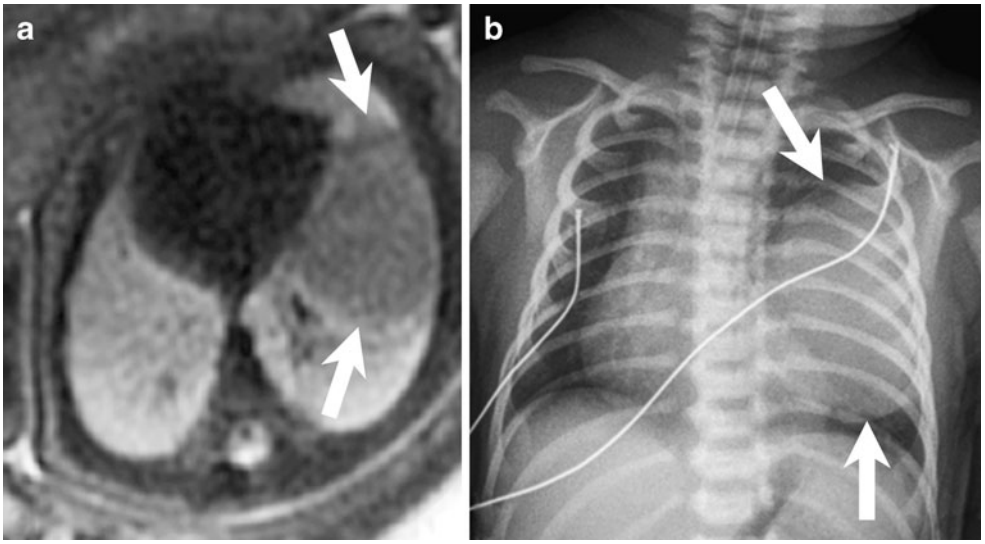

Fig. 18 Congenital pulmonary fibrosarcoma. **a** Axial plane MRI scan through the fetal chest at 25 weeks' gestational age demonstrates a low signal mass (*arrows*) on a fluid-sensitive sequence, consistent with a fibrous tumor. **b** Chest radiograph of the newborn demonstrates a large mass in the left chest (*arrows*) displacing the heart to the right

can undergo torsion, resulting in venous and lymphatic obstruction. This can result in a tension hydrothorax, which, if untreated, may lead to fetal hydrops (Fig. 6) [29].

It is important to note that CLO is not an uncommon cause of a chest mass and has been reported to account for up to 29% of all BPMs [4, 15]. CPAM (a.k.a. CCAM) is often an incorrect default prenatal diagnosis when an echogenic solid mass is detected. Similar to CPAM, CLO can be either lobar or segmental in distribution and receives blood supply from the pulmonary artery [17]. Accurate diagnosis of CLO is important because fetal and postnatal complications are rare compared to those of other BPMs. Most cases are asymptomatic at birth and may be managed conservatively without surgical invention (Fig. 14).

MRI is useful in confirming the presence and size of a mass during the third trimester of pregnancy when solid masses are often not visualized on US (Fig. 13). Accurate assessment of lesion size is important for planning delivery location. When a mass is ascertained to be small, patients can deliver in their local community and undergo elective evaluation of the mass after birth.

The postnatal management of asymptomatic BPMs has been highly controversial, and a complete discussion is beyond the scope of this paper [30–35]. The management debate centers on whether all lesions, irrespective of size, type or symptoms, should undergo surgical resection to prevent the development of known complications, including respiratory distress, infection or, more rarely, pneumothorax. Concern has also been raised regarding the potential for malignant transformation of BPMs, but this is not well-substantiated [36]. Of note, the majority of BPM complications have been reported in association with CPAM and, to a lesser extent, BPS. Long-term postnatal follow-up studies of BPMs are needed to better understand the natural history and help determine optimal management.

In our experience, fetal MRI plays an important role in optimizing the postnatal imaging algorithm. The historical imaging algorithm for a newborn with a prenatally diagnosed chest mass is a chest radiograph, followed by a chest CT scan to confirm and characterize the mass [11]. It is well-recognized that a chest CT scan will usually demonstrate a residual BPM despite a normal chest radiograph in an asymptomatic newborn [37]. Barth et al.

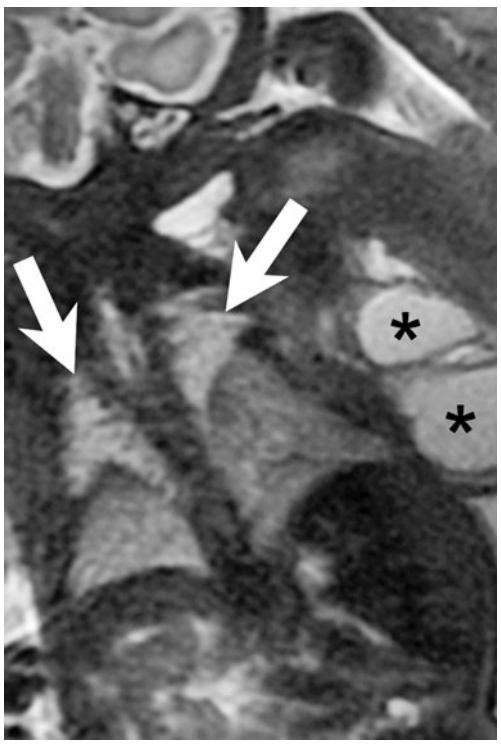

Fig. 19 Lymphatic malformation. **a** Coronal plane MRI through the fetal chest at 28 weeks' gestational age demonstrates a left-side chest wall lymphatic malformation (*asterisks*) with invasion into lung apices manifesting as high signal lesions (*arrows*)

[15] reported concordance between third-trimester MRI and newborn CT scans for the visualization, degree of mediastinal shift and characterization of lung malformations (Fig. 15). The information provided by third trimester fetal MRI has eliminated CT scans in asymptomatic newborns at our institution, thereby reducing newborn radiation exposure and a general anesthetic procedure. When surgical resection is contemplated, a preoperative chest radiograph or CT scan is indicated to confirm the presence of a residual mass. In addition, all malformations require delayed imaging with a chest radiograph or CT, irrespective of symptoms since some malformations, particularly macrocystic CPAMs, may grow postnatally.

Other causes of fetal lung masses

Less common causes of lung masses can be detected in the fetus and are described below.

Congenital high airway obstruction syndrome (CHAOS) occurs secondary to laryngeal atresia, tracheal atresia or a laryngeal cyst. The complete obstruction of the upper airway results in trapping of fluid within the airways and lungs. Prenatal US and MRI demonstrate characteristic imaging features, including dilated central airways, hyperinflated lungs with inversion of the diaphragms and a small heart (Fig. 16). The latter occurs secondary to compression by the hyperinflated lungs. Fetal ascites is a common feature of CHAOS and occurs secondary to a cardiac tamponade effect of the hyperexpanded lungs compressing the heart and inferior vena cava. MRI is useful in showing the precise level of airway obstruction in preparation for the tracheostomy required for postnatal survival (Fig. 16).

Cystic pleuropulmonary blastoma (CPPB) is the most common cause of a primary lung malignancy in childhood. These lesions are macrocystic in the newborn and have been rarely diagnosed in the fetus. The imaging findings both pre- and postnatally are often indistinguishable from those of CPAM (Fig. 17). Findings that may help differentiate a CPPB from a CPAM include a positive family history, multifocal disease, association with a pleural effusion or pneumothorax [36, 38].

Congenital pulmonary fibrosarcoma (a.k.a. congenital peribronchial myofibroblastic tumor) is a rare but distinctive tumor that usually presents as a very large lung mass in the fetus or newborn infant [39]. US features may be atypical for a BPM with a very heterogeneous echotexture. MRI can suggest the correct diagnosis by demonstrating a low signal mass on T1- and T2-weighted sequences, which reflects the high fibrous content within these tumors (Fig. 18). The tumors are benign or of low-grade malignancy. In the absence of metastatic disease, surgical resection is usually curative [39, 40].

Lymphatic malformations typically occur in the posterior or lateral neck. A subset of lymphatic malformations invades the superior mediastinum or lungs manifesting as a high signal mass within the thorax on MRI (Fig. 19). The diagnosis is usually straightforward given the presence of the macrocystic lymphatic malformation outside the chest.

Conclusion

Imaging plays a very important role in predicting outcome, formulating pregnancy management decisions and counseling the family for a fetus with a congenital lung mass. Bronchopulmonary malformations account for the majority of fetal lung masses and are most often detected as an incidental finding on prenatal US. MRI complements US in confirming additional or alternative diagnoses or when US is equivocal.

Disclaimer The supplement this article is part of is not sponsored by the industry. Dr. Barth is a consultant for GE Healthcare and a research grant recipient.

References

1. Kunisaki SM, Fauza DO, Nemes LP et al (2006) Bronchial atresia: the hidden pathology within a spectrum of prenatally diagnosed lung masses. J Pediatr Surg 41:61–65, discussion 61–65
2. Langston C (2003) New concepts in the pathology of congenital lung malformations. Semin Pediatr Surg 12:17–37
3. Riedlinger WF, Vargas SO, Jennings RW et al (2006) Bronchial atresia is common to extralobar sequestration, intralobar sequestration, congenital cystic adenomatoid malformation, and lobar emphysema. Pediatr Dev Pathol 9:361–373
4. Epelman M, Kreiger PA, Servaes S et al (2010) Current imaging of prenatally diagnosed congenital lung lesions. Semin Ultrasound CT MR 31:141–157
5. Stocker JT (2002) Congenital pulmonary airway malformation—a new name for and an expanded classification of congenital cystic adenomatoid malformation of the lung. Histopathology 41:424–431
6. Adzick NS (2003) Management of fetal lung lesions. Clin Perinatol 30:481–492
7. Rosado-de-Christenson ML, Frazier AA, Stocker JT et al (1993) From the archives of the AFIP. Extralobar sequestration: radiologic-pathologic correlation. Radiographics 13:425–441
8. Stocker JT (1986) Sequestrations of the lung. Semin Diagn Pathol 3:106–121
9. Fraser RG, Pare JA (1991) Diagnosis of Disease of the Chest. W. B. Saunders Company, Philadelphia
10. Lager DJ, Kuper KA, Haake GK (1991) Subdiaphragmatic extralobar pulmonary sequestration. Arch Pathol Lab Med 115:536–538
11. Winters WD, Effmann EL (2001) Congenital masses of the lung: prenatal and postnatal imaging evaluation. J Thorac Imaging 16:196–206

12. Newman B (2006) Congenital bronchopulmonary foregut malformations: concepts and controversies. Pediatr Radiol 36:773–791
13. Biyyam DR, Chapman T, Ferguson MR et al (2010) Congenital lung abnormalities: embryologic features, prenatal diagnosis, and postnatal radiologic-pathologic correlation. Radiographics 30:1721–1738
14. Stigers KB, Woodring JH, Kanga JF (1992) The clinical and imaging spectrum of findings in patients with congenital lobar emphysema. Pediatr Pulmonol 14:160–170
15. Barth RA, Newman B, Rubesova E et al (2009) Congenital lobar overinflation (CLO)/congenital lobar emphsysema (CLE)—not an uncommon cause for a fetal chest mass. Pediatr Radiol 39(Suppl 2): S255
16. Kasprian G, Balassy C, Brugger PC et al (2006) MRI of normal and pathological fetal lung development. Eur J Radiol 57:261–270
17. Levine D, Barnewolt CE, Mehta TS et al (2003) Fetal thoracic abnormalities: MR imaging. Radiology 228:379–388
18. Pacharn P, Kline-Fath B, Brody AS et al (2009) Congenital lung lesions: comparison between prenatal magnetic resonance imaging (MRI) and postnatal findings. 95th Scientific Assembly and Annual Meeting. Radiological Society of North America, Chicago, p 186
19. Hubbard AM, Adzick NS, Crombleholme TM et al (1999) Congenital chest lesions: diagnosis and characterization with prenatal MR imaging. Radiology 212:43–48
20. Abdullah MM, Lacro RV, Smallhorn J et al (2000) Fetal cardiac dextroposition in the absence of an intrathoracic mass: sign of significant right lung hypoplasia. J Ultrasound Med 19:669–676
21. Adzick NS, Harrison MR, Crombleholme TM et al (1998) Fetal lung lesions: management and outcome. Am J Obstet Gynecol 179:884–889
22. Crombleholme TM, Coleman B, Hedrick H et al (2002) Cystic adenomatoid malformation volume ratio predicts outcome in prenatally diagnosed cystic adenomatoid malformation of the lung. J Pediatr Surg 37:331–338
23. Miller JA, Corteville JE, Langer JC (1996) Congenital cystic adenomatoid malformation in the fetus: Natural history and predictors of outcome. J Pediatr Surg 31:805–808
24. Duncombe GJ, Dickinson JE, Kikiros CS (2002) Prenatal diagnosis and management of congenital cystic adenomatoid malformation of the lung. Am J Obstet Gynecol 187:950–954
25. Illanes S, Hunter A, Evans M et al (2005) Prenatal diagnosis of echogenic lung: evolution and outcome. Ultrasound Obstet Gynecol 26:145–149
26. Azizkhan RG, Crombleholme TM (2008) Congenital cystic lung disease: contemporary antenatal and postnatal management. Pediatr Surg Int 24:643–657
27. Morris LM, Lim FY, Livingston JC et al (2009) High-risk fetal congenital pulmonary airway malformations have a variable response to steroids. J Pediatr Surg 44:60–65
28. Peranteau WH, Wilson RD, Liechty KW et al (2007) Effect of maternal betamethasone administration on prenatal congenital cystic adenomatoid malformation growth and fetal survival. Fetal Diagn Ther 22:365–371
29. Hernanz-Schulman M, Stein SM, Neblett WW et al (1991) Pulmonary sequestration: diagnosis with color Doppler sonography and a new theory of associated hydrothorax. Radiology 180:817–821
30. Aziz D, Langer JC, Tuuha SE et al (2004) Perinatally diagnosed asymptomatic congenital cystic adenomatoid malformation: to resect or not? J Pediatr Surg 39:329–334
31. Davenport M, Warne SA, Cacciaguerra S et al (2004) Current outcome of antenally diagnosed cystic lung disease. J Pediatr Surg 39:549–556
32. Laje P, Liechty KW (2008) Postnatal management and outcome of prenatally diagnosed lung lesions. Prenat Diagn 28:612–618
33. Kv L, Teitelbaum DH, Hirschl RB et al (1999) Prenatal diagnosis of congenital cystic adenomatoid malformation and its postnatal presentation, surgical indications, and natural history. J Pediatr Surg 34:794–799
34. Sueyoshi R, Okazaki T, Urushihara N et al (2008) Managing prenatally diagnosed asymptomatic congenital cystic adenomatoid malformation. Pediatr Surg Int 24:1111–1115
35. Wong A, Vieten D, Singh S et al (2009) Long-term outcome of asymptomatic patients with congenital cystic adenomatoid malformation. Pediatr Surg Int 25:479–485
36. Priest JR, Williams GM, Hill DA et al (2009) Pulmonary cysts in early childhood and the risk of malignancy. Pediatr Pulmonol 44:14–30
37. Winters WD, Effmann EL, Nghiem HV et al (1997) Disappearing fetal lung masses: importance of postnatal imaging studies. Pediatr Radiol 27:535–539
38. Naffaa LN, Donnelly LF (2005) Imaging findings in pleuropulmonary blastoma. Pediatr Radiol 35:387–391
39. Dishop MK, Kuruvilla S (2008) Primary and metastatic lung tumors in the pediatric population: a review and 25-year experience at a large children's hospital. Arch Pathol Lab Med 132:1079–1103
40. Scheier M, Ramoni A, Alge A et al (2008) Congenital fibrosarcoma as cause for fetal anemia: prenatal diagnosis and in utero treatment. Fetal Diagn Ther 24:434–436